Folate ameliorates arrhythmia in patient-derived TANGO2-deficient iPSC-cardiomyocytes

Lilei Zhang (lileiz@bcm.edu)
Baylor College of Medicine https://orcid.org/0000-0001-6320-1318
Weiyi Xu
Baylor College of Medicine
Yingqiong Cao
Baylor College of Medicine
Andy Yu
Baylor College of Medicine
Jean Kim
Baylor College of Medicine https://orcid.org/0000-0003-4709-262X
Seema Lalani
Baylor College of Medicine
Christina Miyake
Baylor College of Medicine

Brief Communication

Keywords:

Posted Date: June 22nd, 2022

DOI: https://doi.org/10.21203/rs.3.rs-1778084/v1

Abstract

TANGO2-deficient disorder (TDD) is an autosomal recessive genetic disease caused by biallelic loss-of-function variants in *TANGO2* gene. TDD-associated cardiac arrythmias are typically recalcitrant to standard antiarrhythmic medications and constitute the leading cause of death. Here, we established novel patient-derived induced pluripotent stem cell differentiated cardiomyocyte (iPSC-CM) models that recapitulate key electrophysiological abnormalities in TDD including prolonged field potential duration, premature ventricular contractions, and decreased spike amplitude. These conduction abnormalities normalize in iPSC-CMs with either adenoviral expression of WT-TANGO2 or correction of the pathogenic variant by CRISPR editing. We further demonstrate that folate greatly abolishes the ventricular ectopy and conduction abnormalities. Data from this study taken together with clinical data from TDD patients supports the use of B-vitamins to mitigate cardiac crisis in TDD patients.

Main Text

Bi-allelic loss-of-function variants in *TANGO2* (Transport and Golgi organization 2 homolog) cause TANGO2-deficiency disorder (TDD, OMIM #616878), a rare multiorgan disorder associated with significant morbidity[1–14]. While chronic symptoms are predominantly neurodevelopmental, metabolic stressors such as fasting, dehydration, illness, and excessive heat can trigger episodic metabolic crises characterized by encephalopathy, ataxia, muscle weakness, rhabdomyolysis, and hypoglycemia. During these events, patients can develop acute life-threatening cardiac arrhythmias. Electrocardiograms demonstrate marked QTc prolongation and intermittent type I Brugada pattern[13,15]. Arrhythmias typically initiate with isolated premature ventricular contractions (PVC) followed by recalcitrant ventricular tachycardia. Because these lethal arrhythmias usually do not respond to standard antiarrhythmic therapies, cardiac arrhythmias are the leading cause of death in TDD[15–17].

The molecular mechanism of TDD remains largely unclear with conflicting hypotheses[2,5,13,14,18], effective treatment strategies for TDD are lacking and mortality from cardiac arrhythmias is high[15]. Therefore, a cardiac model that recapitulates key electrophysiological abnormalities in TDD is urgently needed to investigate disease mechanism and identify novel therapeutic strategies to ameliorate the high mortality rates.

We generated two independent patient-derived iPSC-CM lines (TAN016 and TAN002). TAN016 is derived from a TDD subject harboring homozygous exons 3–9 deletion (ΔE3-9), the most common variant seen in TDD patients (Fig. 1a). TAN002 harbors homozygous c.460G > A (p.G154R) variant, the most common recurring variant among subjects with Hispanic/Latino ancestry[3]. Both patients developed prolonged QTc during metabolic crisis (Extended Data Fig. 1). TAN002 also demonstrated a Brugada pattern, short pauses, and frequent premature ventricular contractions prior to the onset of lethal ventricular arrythmias[15].

We established isogenic control lines for both TAN016 and TAN002 iPSC-CMs. In TAN016, ΔE3-9 leads to an in-frame deletion resulting in transcription of exon 1–2 only (Fig. 1b), and no translation of full length TANGO2 protein (First lane on the left in Fig. 1c). Thus, we consider the TAN016 iPSC-CMs as a de facto TANGO2-KO line. We then generated a set of 2 isogenic iPSC-CMs on the TAN016 background by expressing WT-TANGO2 or GFP control using an adenoviral vector (TAN016 + Ad-WT or TAN016 + Ad-GFP) (Fig. 1c). For TAN002 (G154R), an isogenic correction line denoted as TAN002c was generated by CRISPR/Cas9-meditated genome editing (Fig. 1d). All four iPSC-CMs lines exhibited spontaneous contraction and positive staining for cardiac sarcomeric proteins such as α-actinin and cardiac troponin T (cTnT) (Extended Fig. 2).

To investigate if these patient-derived iPSC-CMs recapitulate TDD-associated arrhythmia crises, we recorded their spontaneous contraction and extracellular field potential (FP)[19]. We found that TAN016 + Ad-GFP exhibited prolonged FP duration corrected by heart rate (cFPD) (Fig. 1e,f), consistent with prolonged QTc seen in all TDD patients during crisis[15]. In addition, bradycardia and reduced FP spike amplitude were seen (Fig. 1e,g). These findings suggest loss-of-function of the cardiac sodium channel, the molecular etiology of type I Brugada pattern seen in Brugada patients and reported in many patients during TDD crisis including TAN002[15]. Expression of WT-TANGO2 (TAN016 + Ad-WT) but not GFP completely rescued these arrhythmias (Fig. 1e,f,g), confirming these arrhythmias were indeed due to the loss of functional TANGO2. Moreover, the TAN016 + Ad-GFP exhibited frequent premature ventricular contractions (PVCs) (Fig. 2a Left panel), while the TAN016 + Ad-WT showed normal heart rhythm with no PVCs (N = 8; Fig. 2a right panel). Consistently, TAN002 (G154R) displayed cFPD prolongation compared to TAN002c (Fig. 1i). In addition, frequent PVCs as well as pounced intermittent pauses (Fig. 2d Left panel) were observed in TAN002, but not in TAN002c (N = 8; Fig. 2d Right panel). Collectively, these data showed that our patient-derived iPSC-CMs models faithfully recapitulated key arrhythmic phenotypes in TDD.

Although the exact molecular function of TANGO2 and the etiology of TDD remain unclear, data from our Natural history study (ClinicalTrials.gov Identifier: NCT05374616) strongly suggests that subjects on a multivitamin or a B-complex vitamin supplement have a greatly reduced risk for metabolic crises and cardiac arrhythmias (Fig. 1i). In particular, four subjects in our natural history study who are taking folate supplementation without B-complex or multivitamin, 3 of whom are now adults between the ages 20–30 years and have never had a life-time crisis, while the median age at first cardiac arrhythmia crisis was 5.0 years[15]. Moreover, previous studies suggested TANGO2 is important for mitochondrial function and/or protein trafficking from the endoplasmic reticulum (ER) to Golgi aparatus[2,3,14]. Folate, a B vitamin, has been reported to improve both mitochondrial function[20] and ER stress response[21] in murine cardiomyocytes. Therefore, folate was chosen as the candidate effective component of B-complex to test in our iPSC-CMs models. We chose the TAN016 + Ad-GFP model with frequent PVCs to monitor the effect of folate treatment in real time. Strikingly, we found 100mg/L folate, which is 100 times higher than the folate levels in the culture medium greatly ameliorated the occurrence of PVCs (Fig. 2a Middle panel). A decline in PVC frequency is first seen 4 hours after folate treatment, and a complete abolishment of PVCs was observed after 12hrs (Fig. 2b). Interestingly, we also noted that the amelioration of PVCs by folate treatment was associated with a trend of increasing heart rate (Fig. 2c). However, folate does not significantly affect the cFPD compared to that of the vehicle group (Fig. 2d).

We next sought to validate the effect of folate in TAN002 harboring the G154R mutation. Remarkably, both PVCs and pauses were rescued completely by folate (Fig. 2e Middle panel). A single dose of folate reduced PVC burden in TAN002 to almost zero after 3 hours of folate treatment with effects lasting at least 12 hours before PVCs recurred (Fig. 2f, Extended Fig. 3a). Pauses are also eliminated by folate, as demonstrated by the drastic reduction of maximum and variations of inter-beat interval (Extended Data Fig. 3b,c,d). Again, we observed a significant increase in heart rate of TAN002 from 3 to 12hrs after administration of folate compared to that of 0hr, which was not observed in TAN002c with folate (Fig. 2g). It is possible that the beneficial effect from folate is associated with the increase in heart rate in TANGO2-deficienct iPSC-CMs; this is concordant with strategies such as rapid atrial pacing and isoproterenol that have been attempted to treat TDD cardiac crises[15,16]. In addition, folate does not significantly alter the cFPD in TAN002 or TAN002c (Extended Fig. 3e,f), which is consistent with what was observed in TAN016, suggesting folate does not reduce QTc prolongation.

In summary, we established patient-derived iPSC-CMs from two independent genetic backgrounds that carry either homozygous mutations of ΔE3-9 (TAN016) or G154R (TAN002), which account for the largest portion of TDD

affected patients. The two TANGO2-deficient iPSC-CMs lines successfully recapitulated key arrhythmic phenotypes in TDD, including prolonged QT, reduced spike amplitude and frequent PVCs which were abolished in isogenic corrected lines by expression of WT-TANGO2 using an adenoviral vector or CRISPR editing. Our natural history study suggests one or multiple components of the B vitamin complex may be associated with reduced risks for metabolic crises and arrhythmia in TDD patients. Using our novel cardiac models, we demonstrated that folate greatly abolished the PVCs in both TAN016 and TAN002 lines and eliminated pauses in TAN002. This result provided the first experimental evidence supporting the beneficial effects of B-complex for TDD patients. Interestingly, the prolong QT was not rescued by folate, suggesting cardiac Ca^{2+} or K^{+} channels are unlikely to be the downstream effector of folate, but they may still be involved in TDD crisis. The elimination of PVCs by folate coincides with an increase in heart rate only in the TANGO2-deficient iPSC-CMs. A previous study suggested that enhanced connexin 43 expression level in iPSC-CMs elevated the cell excitability and spontaneous beating rate by recruiting additional SCN5A protein expression to the membrane[22]. Collectively, we speculate that multi-channel defects may be present in TDD patient. SCN5A or connexin 43 may be involved in mediating the folate effect, and may be the driving the arrhythmogenic channels in TDD crises. We believe our patient-derived iPSC-CMs model serves as a valuable platform for investigating the mechanism of cardiac arrhythmias and for identifying novel therapies for TDD. Folate and other B vitamins may help reduce the risk for metabolic crises and terminate lethal cardiac arrhythmias in TDD patients.

Declarations

Acknowledgements

We thank Human Stem Core at Baylor College of Medicine for generating all the iPSC lines. We are grateful to the TANGO2 Research foundation for supporting and providing funding for the study. L.Z. is supported by NIH HL143067 and HL150589.

Author contributions

S.R.L, C.Y.M, and L.Z. conceived the project. W.X. and L.Z. designed all the experiments. W.X. and Y.C. performed all the experiments. W.X. and A.C.Y. performed data analysis. W.X., S.R.L, C.Y.M, and L.Z. prepared the figures and wrote the manuscript.

Competing interests

The authors declare no competing interests.

Methods

Patient information

TAN016 is currently an 8-year-old non-Hispanic White female with a history of three metabolic crisis between the ages of 4-6 months of age. During her crisis she developed prolonged QTc and cardiomyopathy. Since starting supplemental formula which contains all B-vitamins including folate, she has not had a subsequent crisis.

TAN002 is currently an 11-year-old Hispanic male with a history of 3 metabolic crisis at the age of 7 years. During his crisis, he developed prolonged QTc, type I Brugada pattern, cardiomyopathy and life-threatening ventricular arrhythmias that responded to isoproterenol. He has not had any recurrent crisis since being initiated on supplemental formula and multivitamins containing folate.

Natural history study

The TDD natural history has been ongoing since February 2019 and is approved by the Institutional Review Board of Baylor College of Medicine (# H-43240). Diagnosis was confirmed by genetic testing or if deceased prior to genetic testing were included based on confirmatory genetic testing of a sibling or parental carrier status. Data from 60 enrolled TDD subjects was collected using questionnaire-based interviews conducted by video or phone with interpreters as necessary and available medical records including metabolic crisis and supplemental vitamin intake. Metabolic crisis was defined as a hospital admission associated with rhabdomyolysis and elevated creatine kinase (CK) above normal range. Cardiac crisis was defined as the development of ventricular arrhythmias, cardiomyopathy, or cardiac arrest during a metabolic crisis.

Generation and maintenance of iPSCs

iPSC reprogramming was performed by Human Stem Cell Core in Baylor College of Medicine following a published protocol[23]. Slight modification was made where ReproTeSR™ Medium (STEMCELL Technologies, #05926) was used during the first week of culture and then switched to mTeSR™1 (STEMCELL Technologies, #85850) for initial expansion. Primary skin fibroblasts from a 7-month-old and 8-year-old TANGO2 patients were provided by Dr. Lalani and used to generate TAN016 and TAN002 iPSC lines, respectively. TAN002c was generated from TAN002 by CRPISR editing. The wild-type iPSC line was reprogrammed using peripheral blood mononuclear cells (PBMCs)[24] from a 37-year-old healthy female donor, which has been registered as BCMi002-A in hPSCreg at https://hpscreg.eu/. All iPSC lines have passed quality control for pluripotency test, karyotyping, and mycoplasma test.

iPSCs were seeded on surface coated with hESC-Qualified Matrigel (Corning, #354277) and maintained in mTeSR™1 or mTeSR™ Plus medium (STEMCELL Technologies, #100-0276). iPSCs were dissociated with ReLeSR™ (STEMCELL Technologies, #05872) or Gentle Cell Dissociation Reagent (STEMCELL Technologies, #100-0485) for regular passage in cell clumps. For passage in single cells, iPSCs were dissociated with Accutase (Innovative Cell Technologies, #AT104) or Accumax (Innovative Cell Technologies, #AM105) and seeded in medium supplemented with 10 μM Y-27632 (MedChemExpress, HY-10071). Y-27632 was removed from the medium after 24hr.

Generation of TAN002c by CRISPR editing

500K singularized TAN002 iPSCs were resuspended in the Lonza nucleofection P3 primary cell solution (Lonza, #V4XP-3024), with 100 picomoles of sgRNA (Synthego), 20 picomoles of Alt-R® S.p. HiFi Cas9 Nuclease V3 (Integrated DNA Technologies, #1081060), and 2 μg of template ssODN (Integrated DNA Technologies) for homology directed repair. RNP was allowed to form in P3 solution for at least 5 min at room temperature, and the nucleofection mixture was loaded into the 16-well nucleocuvette with the total volume less than 25 μl. Electroporation was

performed in the 4D-Nucleofector X Unit (Lonza, #AAF-1003X) using program CB-150 or CA-137. iPSCs were immediately transferred into culture medium supplemented with 10 μM Y-27632 after nucleofection. individual colonies were subsequentially isolated for genotyping and quality check. Sequences of sgRNA and ssODN used are listed below: sgRNA: 5'- CAGCGCGUUGCUCAGCCUGU-3'; template ssODN for homology directed repair: 5'-CTCTGCATGGCCCGCTGATTGCTCCTCACAGGCACCTACGGGCTGAGCAACGCGCTGCTGGAGACTCCCTGGAGGAAGCT-3'.

Differentiation, maintenance, and expansion of iPSC-CMs

We differentiated iPSCs into cardiomyocytes following published protocols [25,26]. Briefly, for induction on day 0, medium was changed to RPMI1640 (Thermo Fisher Scientific, #11875119) with B27 supplement minus insulin (Thermo Fisher Scientific, #17504001) and 8 or 10 μM CHIR99021 (Cayman Chemical, #13122). On day 1, medium was changed to RPMI1640+B27 minus insulin. On day 3, half volume of the medium was changed to RPMI1640+B27 minus insulin supplemented with a final concentration of 5 μM IWP-2 (Cayman Chemical, #13951). On day 5, medium was changed to RPMI1640+B27 minus insulin. Starting from day 7, RPMI1640 with B27 supplement (Thermo Fisher Scientific, #17504001) was used for maintenance of iPSC-CMs and changed every 3 days. Spontaneous contraction was typically observed on day 7. iPSC-CMs were further enriched by lactate selection[27] using glucose-free RPMI1640 (Thermo Fisher Scientific, #11879020) supplemented with 4 mM lactate (MilliporeSigma, L7022) from day 20-24. Some iPSC-CMs were generated using STEMdiff™ Ventricular Cardiomyocyte Differentiation Kit (STEMCELL Technologies, #05010) with similar differentiation efficiency over 85%. iPSC-CMs were further expanded by RPMI1670+B27 supplemented with 2 μM CHIR99021[28]. Expansion was terminated by removal of CHIR99021 in the medium.

Generation of adenovirus

Adenoviruses expressing WT-TANGO2, G154R-TANGO2, and EGFP were generated and tittered by VectorBuilder. The viral construct contains coding sequence of WT or G154R-hTANGO2 with 3XFLAG tag at the C-terminus. The expression was driven under an EF-1α promoter. Adenovirus infection on iPSC-CMs was performed with MOI=1 for all experiments.

DNA extraction, RNA extraction and reverse transcription

Genomic DNA was extracted using QIAamp DNA Mini Kit (Qiagen, #51304). RNA was extracted using high pure RNA isolation kit (Roche, 11828665001). Reverse transcription was performed using iScript™ Reverse Transcription Supermix (Bio-Rad Laboratories, 1708841).

Genotyping and Sanger Sequencing

Primer pairs targeting exon 1-2 (Forward: 5'-CAGGCTGCTTGAAGACCTCG-3'; Reverse: 5'-ACGCGTTTTTGGAAACAGGG-3') and exon 7-8 (Forward: 5'-CAACAATGAAGAGGCGCAGC-3'; Reverse: 5'-

GTACTTGCTCAGCATGGGCTG-3') of human *TANGO2* transcript (ENSG00000183597) were used to genotype the deletion mutation from exon 3-9 deletion in TAN016 using RT-PCR. cDNA from TAN016 and the WT iPSC-CMs (BCMi002-A) were used as templates for PCR. The PCR products were separated in a 2% agarose gel and imaged by ChemiDoc™ Touch Imaging System (Bio-rad Laboratories). Detections of exon 1-2 and exon 7-8 were indicated by 105bp and 82 bp amplicons, respectively.

Sanger sequencing was performed to confirm the G154R mutation in TAN002 and correction in TAN002c. PCR was carried out in Platinum™ SuperFi II Green PCR Master Mix (Thermo Fisher Scientific, #12369010) with a primer pair (Forward: 5'-TCTCCTTGCCATGCCATCAG-3'; Reverse: 5'-CCCACTCACGCCTCTTCATT-3') to amplify a region containing the G154R/correction site from the genomic DNA. The PCR product was purified by PCR purification kit (Zymo Research, D4013) and sent to Azenta Life Sciences for Sanger sequencing. PCR primers along with two additional internal primers (5'-CTGGCAGCACTCACCAACTA-3'; 5'-CAGCTGCGCCTCTTCATTG-3') were used as sequencing primer to ensure specificity. All primers used in the study were synthesized by Integrated DNA Technologies.

Immunoblotting

We lysed iPSC-CMs in RIPA buffer (Thermo Fisher Scientific, #89901) supplemented with protease inhibitor cocktail (Roche, #11836153001). Protein concentration was determined using BCA assay kit (Thermo Fisher Scientific, #23225). Protein samples were mixed with LDS sample buffer (Thermo Fisher Scientific, #B0008) and reducing agent (Thermo Fisher Scientific, #B0009), and then incubated at 70°C for 10min. Proteins were separated on Bolt™ 4-12% Bis-Tris gels (Thermo Fisher Scientific, #NW04122BOX) with MES SDS running buffer (Thermo Fisher Scientific, #B0002). Resolved proteins were then transferred to 0.2µm PVDF membrane (Bio-rad, 1704272) by semi-dry transfer at 25V (up to 1A) for 30min using Trans-Blot® Turbo™ Transfer System (Bio-rad, #1704150). PVDF membrane was then blocked with 5% nonfat milk (Bio-rad, #1706404) in tris-buffered saline with 0.1% Tween (TBST) for 1hr at room temperature. The membrane was then incubated with primary antibody at 4°C overnight and then with mouse anti-rabbit IgG-HRP secondary antibody (Santa Cruz Biotechnology, #sc-2357) at room temperature for 1hr. Enhanced chemiluminescence substrate of HRP (Thermo Fisher Scientific, #34580 or #34094) was used for detection. Na^+/K^+ ATPase (NKA) was used as internal control to avoid possible overlapping with the TANGO2 bands. Primary antibodies used are listed as below: anti-TANGO2 (Proteintech, 27846-1-AP)[13] and anti-NKA (Cell Signaling Technologies, #3010). Both were used at 1:1000 dilution.

Immunofluorescent staining

We dissociated iPSC-CMs by 0.25% Trypsin-EDTA (Thermo Fisher Scientific, 25200072) or STEMdiff™ Cardiomyocyte Dissociation Kit (STEMCELL Technologies, 05025). They were then resuspended in RPMI1640 supplemented with B27, 10% KnockOut™ Serum Replacement (Thermo Fisher Scientific, 10828028), and 10 µM Y-27632 (MedChemExpress, HY-10071), and seeded at 25K per well in 8-well Nunc™ Lab-Tek™ II Chamber Slide™ (Thermo Fisher Scientific, #154453) coated with 2.5 µg/cm^2 of fibronectin (MilliporeSigma, #FC010). Medium was replaced with RPMI1640+B27 two day after seeding for maintenance until further usage. Cells were fixed by 4% PFA in PBS at room temperature for 15min and permeabilized with 0.2% Triton-X in PBS at room temperature for 20min. Slides were then blocked with 5% horse serum (Thermo Fisher Scientific, #16050130) in PBS at room temperature for 2hrs.

Slides were further incubated with primary antibody in 2.5% horse serum PBS at 4 C^o overnight, and then incubated with goat anti-mouse IgG H&L-conjugated with Alexa Fluor® 594 (Abcam, #ab150116) along with DAPI (Thermo Fisher Scientifc, #D3571) at room temperature for 1hr. Images were taken using EVOS FL Auto Imaging System (Thermo Fisher Scientific) under a 20x objective (Thermo Fisher Scientific, #AMEP4734) with light cubes for DAPI (Thermo Fisher Scientific, #AMEP4650) and Texas Red (Thermo Fisher Scientific, #AMEP4655) channels. Primary antibodies used are listed below: anti-α-actinin (MilliporeSigma, #A7811) and anti-cTnT (Abcam, #ab8295). All primary and secondary antibodies were used at 1:500 dilution.

Recording and analysis of contractility and field potential for iPSC-CMs

We seeded iPSC-CMs at 15K per well in 100 µl volume on E-Plate CardioECR 48-well plate (Agilent Technologies, #300601110) coated with 1.875µg/cm^2 of fibronectin. After seeding, iPSC-CMs were maintained for at least 2 weeks before any treatment or adenoviral infection. Folate (MilliporeSigma, #F8758) was freshly prepared at 100 g/L in 1N NaOH (1000X), and further diluted to 5 g/L in RPMI1640+B27 (50X) for better pipetting accuracy. No change in medium pH was observed after administration of the 50X folate solution. The same amount of RPMI1640+B27 was used as vehicle control. As the treatment was performed in a laminar hood and outside the incubator, we observed a 3hr equilibrium time for iPSC-CMs to fully restore the beating rhythm when placed back in the incubator. Therefore, data points between 0-3hr after treatment were not included for analysis.

Cell index and FP were recorded by xCELLigence RTCA CardioECR (Agilent Technologies) in a 37 C^o incubator with 5% CO_2[19]. The duration of each recording was at least 20 seconds. Cell index was recorded by interdigitated impedance microelectrodes that measure the impedance of adherent iPSC-CMs monolayer. Changes in the cell index from baseline indicate contractions of the iPSC-CMs monolayer. Cell index is in arbitrary units. FP signals were recorded by two extracellular FP electrodes in each well, the one with better signal-to-noise ratio was used for analysis. Heart rate, FP spike amplitude, FP duration (FPD), and corrected FPD (cFPD) was calculated by the RTCA CardioECR analysis software (Agilent). Fridericia's formula (FPDc = FPD/inter-spike interval$^{1/3}$) was adopted for correction to minimize influence of a wide range of inter-spike interval FPDs as was suggested in previous publications[29,30]. PVC events were counted manually, and the PVC frequency was calculated as the percentage of PVC counts in total beats in a recording.

A customized MATLAB program was developed to measure inter-beat interval for better accuracy. The raw FP signals were exported from the RTCA CardioECR analysis software. MATLAB was used to construct a notch filter, low pass filter, and wavelet that were applied to reduce the noise of the field potential recording signals. The low pass filter was designed to filter out signals above 120 hertz. A Daubechies 10 wavelet was used to further denoise the signal. Different low pass filter thresholds and wavelets were compared to determine the method which would best reduce background noise while still maintaining signal integrity. After filtering, MATLAB was used to find the peak amplitude value of the FP spike for each waveform. The inter-beat intervals were calculated from the distance between each peak amplitude of each waveform. The mean inter-beat interval, maximum inter-beat interval, minimum inter-beat interval, and standard deviations of inter-beat intervals were calculated for each recording. The MATLAB code for the analysis is available upon request.

References

1. Lalani, S.R., *et al.* TANGO2-Related Metabolic Encephalopathy and Arrhythmias. in *GeneReviews((R))* (eds. Adam, M.P., *et al.*) (Seattle (WA), 2018).
2. Kremer, L.S., *et al.* Bi-allelic Truncating Mutations in TANGO2 Cause Infancy-Onset Recurrent Metabolic Crises with Encephalocardiomyopathy. Am J Hum Genet **98**, 358–362 (2016).
3. Lalani, S.R., *et al.* Recurrent Muscle Weakness with Rhabdomyolysis, Metabolic Crises, and Cardiac Arrhythmia Due to Bi-allelic TANGO2 Mutations. Am J Hum Genet **98**, 347–357 (2016).
4. Karyadi, D.M., *et al.* Whole exome sequencing in 75 high-risk families with validation and replication in independent case-control studies identifies TANGO2, OR5H14, and CHAD as new prostate cancer susceptibility genes. Oncotarget **8**, 1495–1507 (2017).
5. Jennions, E., *et al.* TANGO2 deficiency as a cause of neurodevelopmental delay with indirect effects on mitochondrial energy metabolism. J Inherit Metab Dis **42**, 898–908 (2019).
6. Sen, K., Hicks, M.A., Huq, A.H.M. & Agarwal, R. Homozygous TANGO2 Single Nucleotide Variants Presenting with Additional Manifestations Resembling Alternating Hemiplegia of Childhood-Expanding the Phenotype of a Recently Reported Condition. Neuropediatrics **50**, 122–125 (2019).
7. Dines, J.N., *et al.* TANGO2: expanding the clinical phenotype and spectrum of pathogenic variants. Genet Med **21**, 601–607 (2019).
8. Meisner, J.K., *et al.* Heart Transplantation for TANGO2-Related Metabolic Encephalopathy and Arrhythmia Syndrome-Associated Cardiomyopathy. Circ Genom Precis Med **13**, e002928 (2020).
9. Scuotto, F., *et al.* Electrical storm treated successfully in a patient with TANGO2 gene mutation and long QT syndrome: A case report. HeartRhythm Case Rep **6**, 256–260 (2020).
10. Mingirulli, N., *et al.* Clinical presentation and proteomic signature of patients with TANGO2 mutations. J Inherit Metab Dis **43**, 297–308 (2020).
11. Powell, A.R., Ames, E.G., Knierbein, E.N., Hannibal, M.C. & Mackenzie, S.J. Symptom Prevalence and Genotype-Phenotype Correlations in Patients With TANGO2-Related Metabolic Encephalopathy and Arrhythmias (TRMEA). Pediatr Neurol **119**, 34–39 (2021).
12. Hoebeke, C., Cano, A., De Lonlay, P. & Chabrol, B. Clinical phenotype associated with TANGO2 gene mutation. Arch Pediatr **28**, 80–86 (2021).
13. Berat, C.M., *et al.* Clinical and biological characterization of 20 patients with TANGO2 deficiency indicates novel triggers of metabolic crises and no primary energetic defect. J Inherit Metab Dis **44**, 415–425 (2021).
14. Milev, M.P., *et al.* The phenotype associated with variants in TANGO2 may be explained by a dual role of the protein in ER-to-Golgi transport and at the mitochondria. J Inherit Metab Dis **44**, 426–437 (2021).
15. Miyake, C.Y., *et al.* Cardiac Crises: Cardiac Arrhythmias and Cardiomyopathy during TANGO2-deficiency related Metabolic Crises. Heart Rhythm (2022).
16. Lalani, S., *et al.* TANGO2-Related Metabolic Encephalopathy and Arrhythmias. in *GeneReviews* (2018).
17. Schymick, J., *et al.* Variable clinical severity in TANGO2 deficiency: Case series and literature review. Am J Med Genet A **188**, 473–487 (2022).
18. Heiman, P., *et al.* Mitochondrial dysfunction associated with TANGO2 deficiency. Sci Rep **12**, 3045 (2022).
19. Zhang, X., *et al.* Multi-parametric assessment of cardiomyocyte excitation-contraction coupling using impedance and field potential recording: A tool for cardiac safety assessment. J Pharmacol Toxicol Methods **81**, 201–216 (2016).

20. Piquereau, J., *et al.* Cobalamin and folate protect mitochondrial and contractile functions in a murine model of cardiac pressure overload. J Mol Cell Cardiol **102**, 34–44 (2017).
21. Ye, S., Zhou, X., Chen, P. & Lin, J.F. Folic acid attenuates remodeling and dysfunction in the aging heart through the ER stress pathway. Life Sci **264**, 118718 (2021).
22. Sottas, V., *et al.* Improving electrical properties of iPSC-cardiomyocytes by enhancing Cx43 expression. J Mol Cell Cardiol **120**, 31–41 (2018).
23. Kho, J., *et al.* Argininosuccinate Lyase Deficiency Causes an Endothelial-Dependent Form of Hypertension. Am J Hum Genet **103**, 276–287 (2018).
24. Brookhouser, N., Zhang, P., Caselli, R., Kim, J.J. & Brafman, D.A. Generation and characterization of human induced pluripotent stem cell (hiPSC) lines from an Alzheimer's disease (ASUi001-A) and non-demented control (ASUi002-A) patient homozygous for the Apolipoprotein e4 (APOE4) risk variant. Stem Cell Res **24**, 160–163 (2017).
25. Lian, X., *et al.* Directed cardiomyocyte differentiation from human pluripotent stem cells by modulating Wnt/beta-catenin signaling under fully defined conditions. Nat Protoc **8**, 162–175 (2013).
26. Chi, C., *et al.* LAMP-2B regulates human cardiomyocyte function by mediating autophagosome-lysosome fusion. Proc Natl Acad Sci U S A **116**, 556–565 (2019).
27. Tohyama, S., *et al.* Distinct metabolic flow enables large-scale purification of mouse and human pluripotent stem cell-derived cardiomyocytes. Cell Stem Cell **12**, 127–137 (2013).
28. Buikema, J.W., *et al.* Wnt Activation and Reduced Cell-Cell Contact Synergistically Induce Massive Expansion of Functional Human iPSC-Derived Cardiomyocytes. Cell Stem Cell **27**, 50–63 e55 (2020).
29. Yoshinaga, D., *et al.* Phenotype-Based High-Throughput Classification of Long QT Syndrome Subtypes Using Human Induced Pluripotent Stem Cells. Stem Cell Reports **13**, 394–404 (2019).
30. Yamamoto, W., *et al.* Electrophysiological Characteristics of Human iPSC-Derived Cardiomyocytes for the Assessment of Drug-Induced Proarrhythmic Potential. PLoS One **11**, e0167348 (2016).

Figures

Figure 1

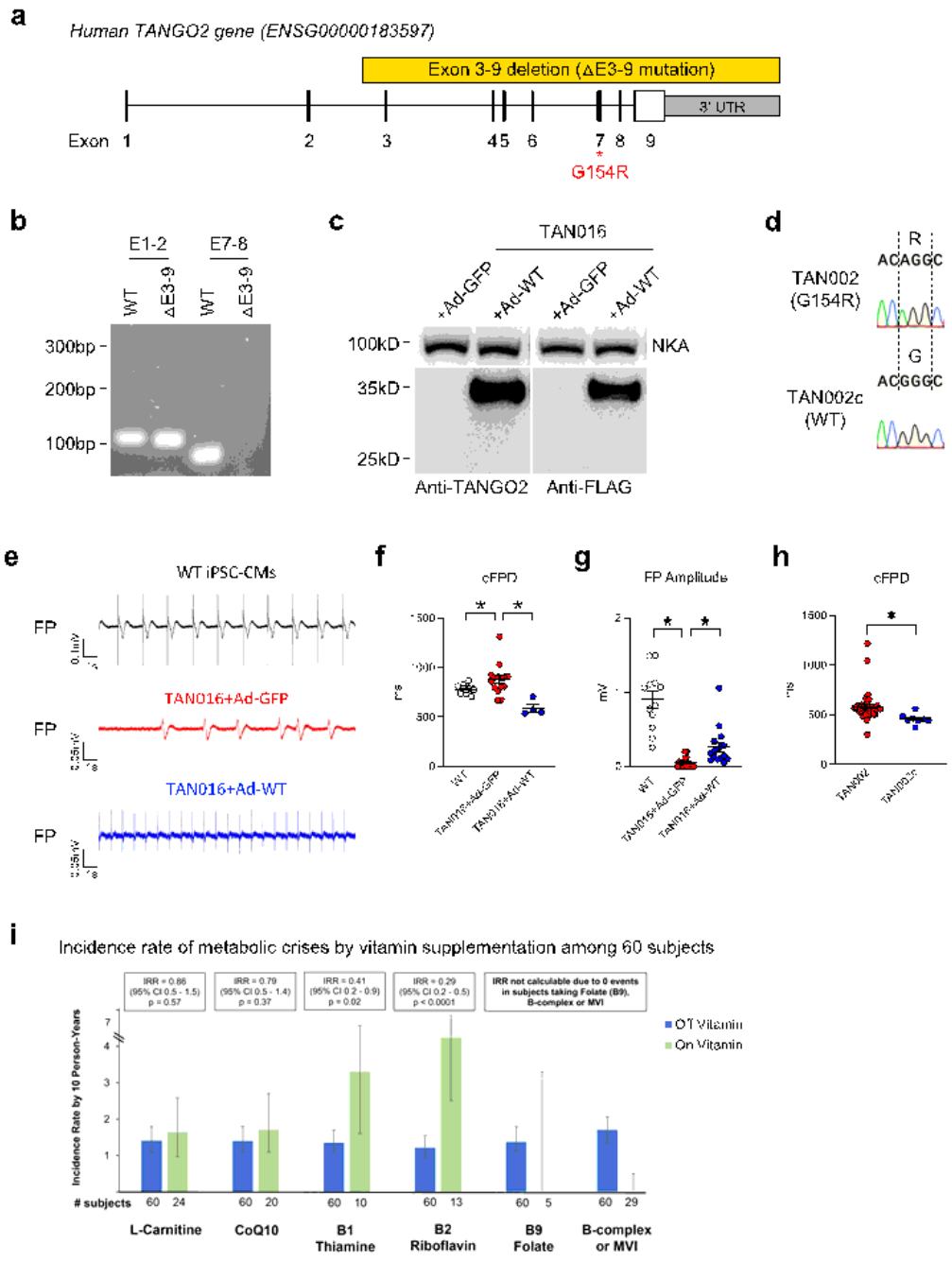

Figure 1

Patient-derived iPSC-CMs models recapitulate arrhythmia in TANGO2-deficient disorder. a, G154R and ΔE3-9 (deletion of Exon 3-9) mutations in human *TANGO2* locus. Coding region in exons are shown in black. **b,** RT-PCR for TAN016 using primer pairs targeting exon 1-2 (E1-2) or exon 7-8 (E7-8) of WT-TANGO2 transcript. Sample from an unrelated WT line was used as positive control. **c,** Western blot showing the adenoviral expression of WT-TANGO2 protein in TAN016 iPSC-CMs. A 3XFLAG tag was added to the C-terminus of the ectopic TANGO2 protein. Image on the right demonstrates the specificity of TANGO2 polyclonal antibody using an anti-FLAG antibody. Na^+/K^+ ATPase (NKA) was used as loading control. **d,** Sanger sequencing confirmed the genotypes in TAN002 and its isogenic correction line TAN002c. **e,** Representative field potential (FP) tracings of an unrelated WT control and TAN016 iPSC-CMs with adenoviral expression of WT-TANGO2 or GFP control. FP indicates the electrical activity of iPSC-CMs. **f,g,**

Quantifications of (f) FPD corrected by heart rate (cFPD) and (g) FP spike amplitude of three iPSC-CM lines in e. **h**, Quantifications of cFPD of TAN002 and TAN002c. *: p<0.05, one-way ANOVA using Dunnett's correction with α=0.05. **i,** Incident rate ratios (IRR) of metabolic crises events is calculated by number of crisis events over patient years when not on a supplement divided by number of events when taking a supplement. Non-B supplements such as L-Carnitine and CoQ10 do not eliminate crisis. In addition, crises continue to occur when subjects take Thiamine (B1) and Riboflavin (B2) alone. Although subject numbers are on folate (B9) alone are small, these subjects have not developed crisis. Metabolic crises events are also eliminated among patients taking B-complex or multivitamins (both contain folate). The IRR for folate, B-vitamins and multivitamins could not be calculated as 0 events were observed among subjects on folate, B-complex or multivitamin supplement.

Figure 2

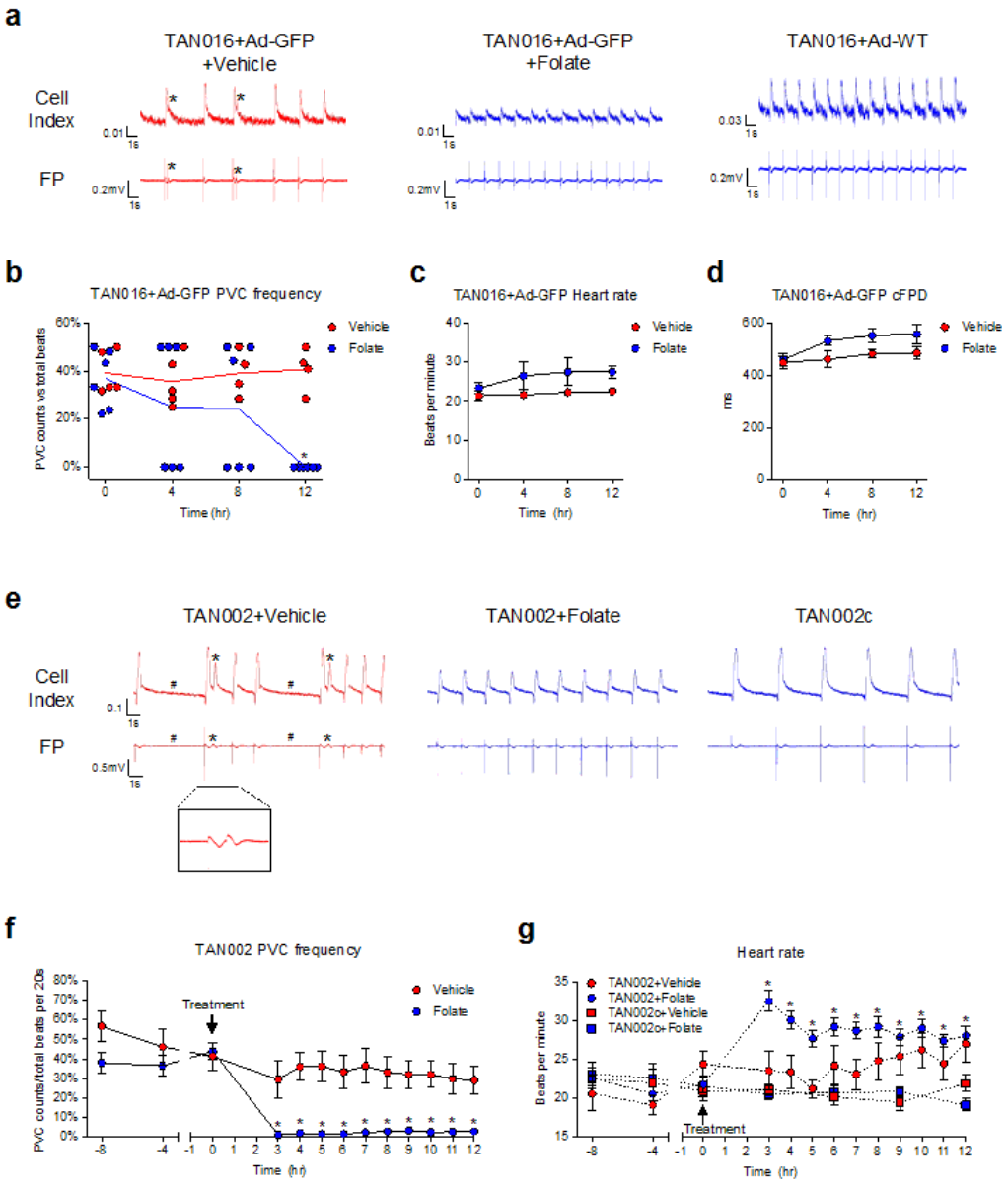

Figure 2

Folate ameliorated arrhythmias in TANGO2-deficient iPSC-CMs. a, Representative recordings of TAN016+Ad-GFP with vehicle or 100mg/L folate for 12hrs. TAN016+Ad WT did not show arrythmia and was not treated. Changes in cell index from baseline represent contractions in arbitrary units. Field potential (FP) shows the corresponding electrical activity. * Indicate PVCs. **b,** Quantification of PVC frequency of TAN016+Ad-GFP with vehicle or folate treatment. PVC frequency was calculated as the percentage of PVC counts in total beats for each recording. Circles indicate individual wells and lines indicate changes of group mean over 12 hours. N=4-6. *p<0.05 vs vehicle. **c,d,** Quantification of (c) heart rate and (d) cFPD over time comparing TAN016+Ad-GFP with vehicle or folate. **e,** Representative tracings of TAN002 treated with vehicle or 100mg/L folate for 4hrs. TAN002c did not show arrhythmia and was not treated. * and # indicate PVCs and pauses, respectively. Inset: a typical PVC event. **f,** Quantification of PVC frequency in TAN002 with vehicle or folate treatment. N=13-43. *p<0.05 vs vehicle. **g,** Heart rate of TAN002 and TAN002c with vehicle or folate treatment. N=13-43. Arrows indicate the administration of treatment. *p<0.05 vs 0hr. Statistical difference is determined by two-way ANOVA corrected by Sidak method with α=0.05. For data in **b,c,e,f**. Data are mean ± SEM. Error bars smaller than the circles are not shown.

Supplementary Files

This is a list of supplementary files associated with this preprint. Click to download.

- Onlinefloatimage3.png
- Onlinefloatimage4.png
- Onlinefloatimage5.png